

RESEARCH

Open Access



Postnatal downregulation of *Fmr1* in microglia promotes microglial reactivity and causes behavioural alterations in female mice

Mehdi Hooshmandi¹, David Ho-Tieng¹, Kevin C. Lister¹, Weihua Cai¹, Calvin Wong¹, Nicole Brown¹, Jonathan Fan¹, Volodya Hovhannisyani¹, Sonali Uttam¹, Masha Prager-Khoutorsky², Nahum Sonenberg³, Christos G. Gkogkas^{4*} and Arkady Khoutorsky^{1,5*}

Abstract

Background Fragile X syndrome is caused by the loss of the *Fmr1* gene expression. Deletion of *Fmr1* in various neuronal and non-neuronal subpopulations in the brain of mice leads to cell-type-specific effects. Microglia, immune cells critical for the refinement of neuronal circuits during brain development, have been implicated in various neurodevelopmental disorders, including fragile X syndrome. However, it is unknown whether reduced *Fmr1* expression in microglia leads to molecular and behavioral phenotypes.

Methods We downregulated *Fmr1* in microglia during early and late postnatal development and studied the effect on microglial morphology and distinct behaviours.

Results Female, but not male, adult mice with downregulation of *Fmr1* in microglia during early development exhibited reactive microglia and behavioral phenotypes, including enhanced self-grooming and alterations in social interaction. Downregulation of *Fmr1* in microglia during late development induced a milder phenotype, characterized by impaired preference for social novelty without affecting microglia morphology.

Conclusions The downregulation of *Fmr1* and its encoded protein FMRP in microglia contributes to behavioural phenotypes in a sex-specific manner.

Keywords *Fmr1*, Microglia, Animal models, Behaviours reminiscent of autism

*Correspondence:

Christos G. Gkogkas
cgkogkas@bri.forth.gr

Arkady Khoutorsky
arkady.khoutorsky@mcgill.ca

¹Department of Anesthesia, Faculty of Dental Medicine and Oral Health Sciences, McGill University, Montreal, QC, Canada

²Department of Physiology, McIntyre Medical Sciences Building, McGill University, Montreal, QC, Canada

³Department of Biochemistry and Goodman Cancer Research Centre, McGill University, Montreal, Canada

⁴Biomedical Research Institute, Foundation for Research and Technology-Hellas, Ioannina, Greece

⁵Alan Edwards Centre for Research on Pain, McGill University, Montreal, QC, Canada



© The Author(s) 2025. **Open Access** This article is licensed under a Creative Commons Attribution-NonCommercial-NoDerivatives 4.0 International License, which permits any non-commercial use, sharing, distribution and reproduction in any medium or format, as long as you give appropriate credit to the original author(s) and the source, provide a link to the Creative Commons licence, and indicate if you modified the licensed material. You do not have permission under this licence to share adapted material derived from this article or parts of it. The images or other third party material in this article are included in the article's Creative Commons licence, unless indicated otherwise in a credit line to the material. If material is not included in the article's Creative Commons licence and your intended use is not permitted by statutory regulation or exceeds the permitted use, you will need to obtain permission directly from the copyright holder. To view a copy of this licence, visit <http://creativecommons.org/licenses/by-nc-nd/4.0/>.

Background

Fragile X syndrome (FXS) is a genetic neurodevelopmental disorder and the leading monogenic cause of intellectual disability and autism [1]. In FXS, expansion of the CGG repeat within the promoter region of the *Fmr1* gene on the X chromosome leads to the transcriptional silencing of the *Fmr1* gene and the subsequent absence of its protein product, fragile X messenger ribonucleoprotein 1 (FMRP) [2]. FMRP is an RNA-binding protein that regulates protein synthesis, mRNA stability, and trafficking [3]. *Fmr1* knockout (KO) mice, which have been widely used to study FXS, exhibit numerous phenotypes reminiscent of FXS, including impaired social interaction and repetitive behaviors [4, 5].

Emerging evidence indicates that FMRP regulates molecular and behavioural phenotypes in a cell-type-specific manner. Deletion of *Fmr1* in forebrain excitatory neurons results in enhanced locomotor activity, anxiety-like behavior, and amplified resting EEG gamma power [6, 7]. Deletion of *Fmr1* in VGlut2-expressing glutamatergic neurons induces audiogenic seizures [8]. *Fmr1* deletion in subpopulations of inhibitory neurons revealed that mice lacking *Fmr1* in parvalbumin-expressing interneurons exhibit dysregulated *de novo* protein synthesis, anxiety-like behavior, and impaired social behavior, whereas mice lacking *Fmr1* in somatostatin-expressing neurons show no changes in protein synthesis or behavior [9]. Deletion of *Fmr1* in cerebellar Purkinje cells results in enhanced long-term depression (LTD) at the parallel fiber synapses, and deficits in delay eyeblink conditioning [10].

Apart from neurons, *Fmr1* is also expressed in non-neuronal cells, such as astrocytes [11, 12] and microglia [13]. Selective ablation of *Fmr1* in astrocytes decreased glutamate transporter GLT1 levels and increased neuronal sensitivity to extracellular glutamate [14]. Microglia are resident immune cells in the brain that play important roles in brain homeostasis, synaptic pruning, and the formation of neuronal circuits during early postnatal brain development [15–17]. Dysregulation of microglial function, including alterations in their activation state and abundance, is observed in postmortem brains of individuals with ASD [18] and *Fmr1* KO mice [19]. Despite the crucial role of microglia in brain development and their involvement in distinct neurodevelopmental disorders [20–22], the role of microglial FMRP in FXS remains unknown. In this study, we downregulated *Fmr1* in microglia during early and late postnatal development in both sexes and assessed behavioural and microglial phenotypes.

Methods

Animals

To generate mice with microglia-specific deletion of *Fmr1*, *Fmr1*^{fl/fl} female mice [23] (kindly provided by

Dr. David L. Nelson, Baylor College of Medicine) were crossed with male mice expressing Cre recombinase under the microglia-specific promoter, TMEM119^{CreERT2} (JAX, stock #031820) [24]. The *Fmr1*^{fl/y} TMEM119^{CreERT2} mice were consequently crossed with *Fmr1*^{+/-} TMEM119^{CreERT2} mice to obtain female *Fmr1*^{fl/fl} TMEM119^{CreERT2} mice. TMEM119^{CreERT2} mice were used as a control group. Mice were housed by genotype. Both experimental and control mice were injected with 4-OHT or tamoxifen, see “Pharmacological reagents” for details. All the mouse strains were maintained on the C57BL/6 background. Adult male and female mice (8-week-old) were used in all experiments. All experiments were conducted and analyzed by a researcher blind to the genotypes and treatments. The animals were housed in standard Plexiglas mouse cages with food and water available *ad libitum* and maintained on a 12-hour light/dark cycle with lights on at 7:00 AM. All procedures were compliant with the Canadian Council on Animal Care guidelines and approved by McGill University’s Animal Care Committee.

Immunohistochemistry

Mice were transcardially perfused with 1X PBS followed by 4% paraformaldehyde (PFA), pH 7.4. Following extraction, the brains were postfixed in PFA 4% for 24 h at room temperature. The fixed brains were then sectioned transversely using a vibratome to acquire 50- μ m-thick sections. After washing with PBS, sections were blocked using 10% normal goat serum (NGS) and 0.5% Triton-X100 in PBS for two hours. The blocking was then followed by an overnight incubation with primary antibodies. For confirmation of FMRP downregulation, FMRP (1:200, Cat No. ab17722, Abcam) and Iba1 (1:500, Cat No. 234–308, Synaptic Systems) were used, and for 3-D image analysis, Iba1 (1:500, Cat No. 019-19741, Wako) and CD68 (1:500, Cat No. MCA1957, Bio-rad) were used in 0.5% Triton-X100 in PBS (PBS-T). After three washes with PBS, sections were incubated for two hours at room temperature with the corresponding secondary antibodies (1:500) diluted in PBS. DAPI (1:5000) was added to the solution in the last wash. Finally, sections were mounted on glass slides, imaged using a confocal microscope (Zeiss LSM 880) with a 63X/1.40 Oil DIC f/ELYRA objective, and images were analyzed using ImageJ (NIH). All images were captured using Z-stack mode with 15–20 optical sections/stack. The integrated density signal within the cell body of Iba1-positive cells in the corpus callosum was quantified using ImageJ on maximum intensity projection images. Two sections per animal were imaged, and the integrated density of FMRP in 5–10 microglia per image was quantified. The values of the total microglia were averaged to obtain a single value per mouse. 3D image analysis of microglia was

performed using IMARIS (See IMARIS section for more details).

Open field test

Mice were individually placed into an illuminated (~1,200 lx) white non-porous plastic square box without bedding (50 cm x 50 cm x 31 cm) and given 10 min to freely explore the apparatus. Their activities were recorded and analyzed using the Noldus EthoVision XT video tracking software. The time spent inside and outside the defined zones (inner zone 33 cm x 33 cm) was then analyzed.

Marble burying test

After a 30-minute habituation period, mice were individually placed in a plexiglass cage (50 cm x 50 cm x 31 cm) filled with 5 cm of bedding. The mice were allowed to bury 18 shiny and clean marbles, which were equally distributed in three rows of 6 marbles, for 30 min. The marble was considered buried if at least 2/3 of it was covered by bedding. The limitation of this analysis is that it does not distinguish whether the marble is buried due to direct burying behaviours or walking/sitting on them in passing.

Self-grooming test

Mice were placed in a mouse cage with fresh bedding and allowed to habituate and explore the cage for 20 min. Grooming behavior during the last 10 min was recorded using an overhead rigged camera. The total time spent on self-grooming, and the number of grooming bouts were scored and analyzed.

Elevated plus maze

To assess anxiety-like behavior, mice were individually placed in the center of the elevated plus maze and allowed to explore for 5 min while their activity was recorded using a mounted camera positioned above the maze. The maze consisted of two open arms (30 cm x 5 cm) and two closed arms (30 cm x 5 cm x 15 cm), elevated 50 cm above ground level. The time spent in the open and closed arms, as well as the total number of arm entries, were calculated and analyzed.

Three-chamber social interaction test

A Plexiglass box with three interconnected compartments (36 cm x 28 cm x 30 cm) was used to assess social interaction and novelty-seeking behavior. In the first 10-minute habituation phase, the test mouse was placed in the middle compartment and was allowed to explore empty small wire cages located in the right and left compartments for 10 min. During the 10-minute sociability phase, the test mouse was exposed to an empty wire cage in one compartment and a wire cage containing a

stranger mouse (Stranger 1, age- and sex-matched wild-type mouse, C57BL/6J) in the other compartment. In the final 10-minute novelty-seeking phase, the test mouse was allowed to explore the wire cage containing the now familiar Stranger 1, and a novel stranger (Stranger 2) confined in the other wire cage. All three phases began with placing the test mouse in the middle compartment and opening doorways to the right and left compartments. The left/right sides of the apparatus were counterbalanced to contain stimuli or empty wire cage across subjects. The light intensity in the room was 255 lx. The entire 30-minute test was recorded using an overhead-mounted camera. The total time spent in each compartment, the time spent in social interaction, and the total number of compartment entries were scored and analyzed. Social interaction time was defined as the time when the test mouse approached the empty or occupied wire cage at a distance of less than 1 cm.

Reciprocal (direct) social interaction test

After habituating mice for five minutes in a novel standard mouse housing cage (27 cm x 15 cm x 12 cm) with fresh corn cob bedding, mice were individually exposed to an unfamiliar age and sex-matched mouse (WT) for 10 min. The recorded video was then analyzed to measure the total time of interaction between the test mouse and the unfamiliar WT mouse (defined as nose-to-anogenital sniffing, nose-to-nose sniffing, and social grooming). The light intensity in the room was 255 lx.

Pharmacological reagents

4-OHT: 4-Hydroxytamoxifen (4-OHT) was first dissolved at 20 mg/ml in ethanol and then further diluted in sunflower oil to obtain a final concentration of 2 mg/ml with 10% ethanol. Mice then received intraperitoneal injections of 4-OHT (Sigma, Cat. No. H7904) once daily for five consecutive days from postnatal day 1 to postnatal day 5, with each animal receiving a total dosage of 0.25 mg. **Tamoxifen:** Tamoxifen (Sigma T5648) was dissolved in 10% ethanol and 90% sunflower oil to obtain 20 mg/ml concentration. Animals then were administered 100 mg/kg of tamoxifen or vehicle intraperitoneally daily for 5 consecutive days starting at postnatal day 30.

IMARIS

To study the morphology and phagocytic activity of microglia, Sholl and CD68 lysosome analyses of microglia were conducted on the hippocampal and cortical sections using IMARIS (9.7.2). Microglia and lysosomal volume were analyzed using Iba1 and CD68 staining, respectively. Thick Sect. (70 µm) of the hippocampus and cortex were used. High-resolution images of individual microglia using a Zeiss LSM 880 upright confocal microscope using a 63X oil objective (NA: 1.4) (38–48 µm z-stacks; xy

resolution: 0.10 μm ; z step: 0.2 μm , 1024 \times 1024 px) were captured. The CZI file format (.czi) was converted into an Imaris file format (.ims) using a file converter, so it could be opened in Imaris 9.7.1. The Filament Tracer Module in IMARIS was used to reconstruct microglia for Sholl analysis, with the Iba1 channel being selected for this purpose. After reconstruction, the filament number of Sholl intersections data were generated by IMARIS and compiled into an Excel spreadsheet for further analysis. Lysosomal volume was measured by 3D reconstruction and overlapping CD68 signal with Iba1. The surface rendering model was utilized to identify microglia and CD68 surfaces for conducting volume-based analysis. Surfaces were reconstructed for CD68 and Iba1 separately. The amount of CD68 volume that colocalizes with the Iba1 signal was analyzed by IMARIS and combined in an Excel spreadsheet before analysis. Two sections per animal were imaged and analyzed. A total of 5–10 cells per section were analyzed. Each group consisted of five mice. IMARIS 3D reconstruction was utilized in conjunction with representative images of Iba1/CD68 to demonstrate the localization of CD68 within microglia.

Statistical analysis

Statistical analysis was conducted using GraphPad Prism 9 (GraphPad Prism Software Inc., USA) and the data were tested for normality using the Shapiro–Wilk test. The data are presented as mean \pm standard error of the mean (s.e.m.), and significance was defined as $p < 0.05$. Differences between two groups were assessed using a two-tailed unpaired Student's *t*-test or a nonparametric two-tailed Mann–Whitney test. Multiple group comparisons were performed using either one-way ANOVA or two-way ANOVA, followed by Tukey's or Bonferroni's post-tests. All behavioral assessments were scored and analyzed by an experimenter blinded to both genotypes and treatments. Each data point in the graphs corresponds to the number of animals.

Results

Microglia-specific downregulation of *Fmr1*

To delete *Fmr1* in microglia, we crossed *Fmr1*^{fl/fl} mice with mice expressing Cre recombinase under the control of the microglia-specific promoter, *Tmem119* (*TMEM119*^{CreERT2}). Male and female *TMEM119*^{CreERT2} mice were used as controls. To target early postnatal development, the experimental and control groups received 4-Hydroxytamoxifen (4-OHT, daily) during postnatal days 1 to 5 (mice referred to as *Fmr1* cKO^{early}, Fig. 1A). For late postnatal development, experimental and control mice were treated daily with tamoxifen from day 30 to 34 (referred to as *Fmr1* cKO^{late}, Fig. 1B). Previous work has reported that FMRP is detected in microglia in all examined brain areas during the first postnatal weeks;

however, its expression is dramatically reduced in adult mice, particularly in the hippocampus and cerebellum [13]. In contrast, the expression of FMRP in microglia remains stable in the corpus callosum across the lifespan [13]. To confirm the downregulation of *Fmr1* in microglia in our cKO mouse models, we measured FMRP expression in corpus callosum microglia of 8-week-old mice using immunohistochemistry with FMRP-specific antibodies and a microglial marker, Iba1. FMRP levels were significantly decreased in microglia of *Fmr1* cKO^{early} (Fig. 1C and D) and *Fmr1* cKO^{late} (Fig. 1E and F) mice.

Early development downregulation of microglial *Fmr1* causes female-specific behavioural alterations and changes in microglial morphology

To study the role of *Fmr1* in microglia during the early developmental stages in the pathogenesis of behaviors reminiscent of fragile X syndrome, adult *Fmr1* cKO^{early} mice underwent behavioural testing. Female *Fmr1* cKO^{early} mice spent less time in the inner zone and more time in the outer zone of the open field test compared to controls (Fig. 2B). Female *Fmr1* cKO^{early} mice also exhibited increased self-grooming time (Fig. 2C) and marble-burying behaviors (Fig. 2D). No anxiety phenotype was observed in the elevated plus maze (Fig. 2E), as no differences were found in the time spent in the open arm or closed arm between the *Fmr1* cKO^{early} and control mice (although a trend was observed). Female *Fmr1* cKO^{early} mice showed deficits in the novelty-seeking phase of the three-chamber social interaction tests (Fig. 2F, right). *Fmr1* cKO^{early} female mice also showed reduced direct social interaction in the reciprocal social interaction test, although it did not reach statistical significance ($p = 0.0704$, Supplemental Fig. 1A). Surprisingly, in contrast to females, male *Fmr1* cKO^{early} mice exhibited no significant deficits in the open field, self-grooming, marble burying, elevated plus maze, and three-chamber social interaction tests (Fig. 2G–K; integrated male and female analyses are shown in Supplemental Fig. 1B–D). These findings indicate that the early postnatal downregulation of *Fmr1* in microglia in female mice is sufficient to induce enhanced self-grooming and alterations in the novelty phase of the three-chamber social interaction test.

We next studied whether the early postnatal downregulation of *Fmr1* in microglia affects the morphology and phagocytic capacity of microglia. The analysis of microglial morphology using 3D reconstruction of Iba1 immunostaining showed that hippocampal and cortical microglia in female *Fmr1* cKO^{early} mice exhibit diminished arborization, as indicated by the reduced number of intersections in 3D Sholl analysis (Fig. 3B, cortex; E, hippocampus), as well as the decreased branch number (Fig. 3C, cortex; G, hippocampus) and processes length

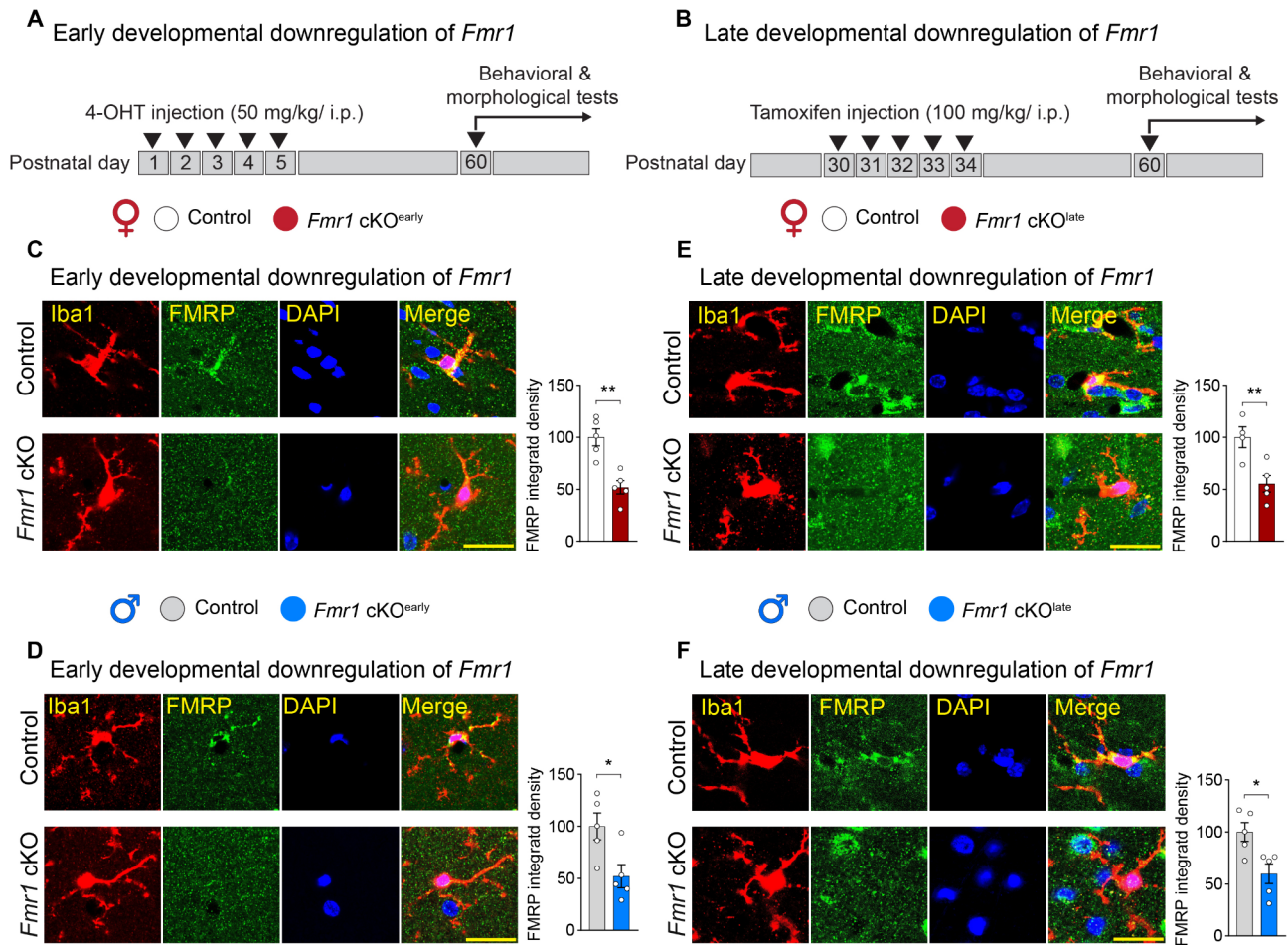


Fig. 1 Downregulation of the *Fmr1* gene in microglia. (**A, B**) The schematics illustrate the early and late developmental downregulation of the *Fmr1* gene induced by either 4-OHT (50 mg/kg/i.p.) or tamoxifen (100 mg/kg/i.p.) administration, respectively. (**C–F**) Immunostaining against FMRP in microglia (Iba1⁺ cells) shows ablation of FMRP in microglia at early and late postnatal developmental stages in the corpus callosum of *Fmr1* cKO^{early} and *Fmr1* cKO^{late} compared to the controls (**C**, Female: *Fmr1* cKO^{early} vs. control, $t_8 = 4.60$, $**p = 0.0018$; **D**, Male: *Fmr1* cKO^{early} vs. control, $t_8 = 2.81$, $*p = 0.0227$, $n = 5$ for all groups) and *Fmr1* cKO^{late} (**E**, Female: *Fmr1* cKO^{late} vs. control, $t_7 = 3.54$, $**p = 0.0094$; **F**, Male: *Fmr1* cKO^{late} vs. control, $t_8 = 3.07$, $*p = 0.0154$, $n = 4–5$). ImageJ was used to quantify the FMRP integrated density signal within the cell body of Iba1-positive cells in the corpus callosum, using maximum intensity projection images. Two sections per animal were imaged, and the integrated density of FMRP in 5–10 microglia per image was quantified. The values were averaged to obtain a single value per mouse. Unpaired two-tailed Student's *t*-test. Data points represent individual mice. Data are shown as mean \pm SEM. The scale bars are 25 μ m. $*p < 0.05$ and $**p < 0.01$

(Fig. 3D, cortex; H, hippocampus). Moreover, volumetric analysis of CD68⁺ signal, indicative of microglial phagocytic capacity, showed a significant increase in CD68/Iba1 volume ratio in the cortex (Fig. 3E) and hippocampus (Fig. 3I) of female *Fmr1* cKO^{early} mice. Conversely, male *Fmr1* cKO^{early} mice exhibited no change in microglia morphology and CD68 volume (Fig. 3K–R). Decreased arborization of microglial processes combined with increased CD68 signal in *Fmr1* cKO^{early} female mice suggests that the early postnatal downregulation of *Fmr1* in microglia induces the transition of microglia to a reactive state in a sex-dependent manner [25].

***Fmr1* ablation in microglia during late development leads to deficits in the novelty-seeking phase of the three-chamber social interaction tests in female mice**

We next tested mice with downregulation of *Fmr1* in microglia during the late stage of development (*Fmr1* cKO^{late}). Female *Fmr1* cKO^{late} mice showed impairment in the novelty-seeking phase of the three-chamber social interaction test (Fig. 4E, right), but no deficits in the sociability phase (Fig. 4E, left), direct social interaction (Supplemental Fig. 1E), open field (Fig. 4B), self-grooming (Fig. 4C), marble burying (Fig. 4D), and elevated plus maze (Fig. 4E) compared to controls. No behavioral alterations were observed in male *Fmr1* cKO^{late} mice (Fig. 4G–K). Notably, late-development downregulation of *Fmr1* in microglia did not affect their reactivity state, as indicated

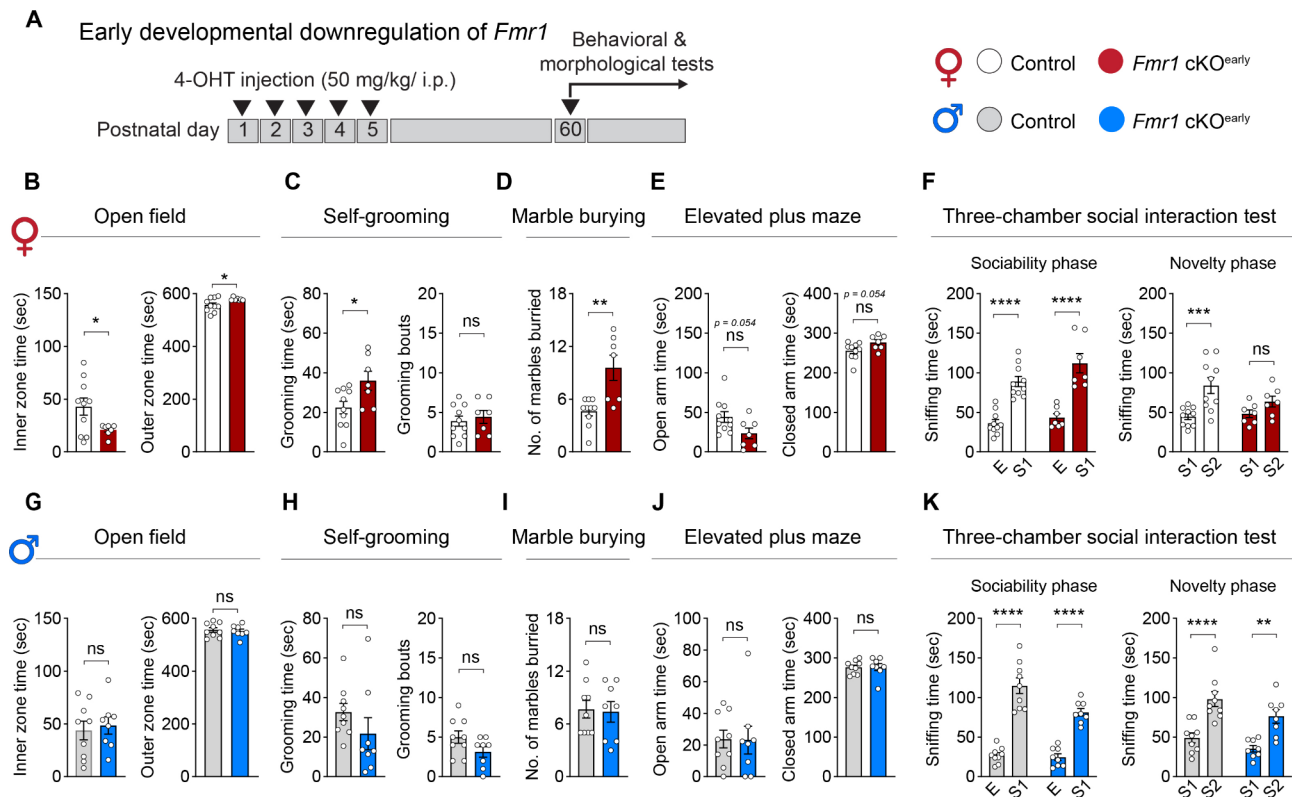


Fig. 2 Early developmental downregulation of microglial *Fmr1* causes sex-specific behavioural alterations (A) Schematic illustration of early deletion of *Fmr1* gene in microglia. (B–F) Behavioral analysis of female *Fmr1* cKO^{early} (KO *n* = 7, Control *n* = 10) showed that the mice spend less time in the inner zone and more time in the outer zone of the open field test (B, inner zone time: *t*₁₅ = 2.20, **p* = 0.0438 and outer zone time: *t*₁₅ = 2.20, **p* = 0.043). Female *Fmr1* cKO^{early} mice spent more time self-grooming (C, *t*₁₅ = 2.44, **p* = 0.0273) and buried more marbles (D, ***p* = 0.0068). No anxiety-like behavior was observed in the elevated plus maze (E, ns, *p* > 0.05). In the three-chamber social interaction test, female *Fmr1* cKO^{early} mice exhibited impaired novelty seeking (F, left: ns, *p* > 0.05), whereas no impairment was observed in the sociability phase of the test (F, right: *t*₃₀ = 5.67, *****p* < 0.0001). (G–K) No significant differences in male *Fmr1* cKO^{early} mice as compared to controls in the open field, self-grooming, marble burying, elevated plus maze, and three-chamber social interaction tests (G–K, ns, *p* > 0.05 for all tests, *n* = 8–9). Unpaired two-tailed Student’s *t*-test was used for B–C, E, and G–I, and two-tailed Mann–Whitney test was used for D and J. The three-chamber social interaction test was analyzed using two-way ANOVA followed by Bonferroni’s multiple comparisons test. Data points represent individual mice. Data are shown as mean ± SEM. **p* < 0.05, ***p* < 0.01, *****p* < 0.0001, ns– not significant

by no alterations in microglial arborization in the cortex and hippocampus of male and female mice, as well as unchanged CD68⁺ volume (Supplemental Fig. 2, A–R). Thus, downregulation of microglial *Fmr1* during the late postnatal stage has no major effect on microglial phenotypes and repetitive behaviours, but it causes deficits in the novelty-seeking phase of the three-chamber social interaction test in female mice.

Discussion

We found that decreasing *Fmr1* in microglia during the early postnatal development is sufficient to induce morphological changes in microglia, along with enhanced self-grooming and deficits in the novelty-seeking phase of the three-chamber social interaction test in adult female, but not male mice. Downregulation of *Fmr1* in microglia during the later developmental stage led to impairments in the novelty-seeking phase of the three-chamber social interaction test, but not self-grooming behavior

or microglial morphology. Thus, we identified a critical postnatal developmental window for FMRP in microglia, linked to sexually dimorphic cellular and behavioral phenotypes.

FMRP expression in microglia across various brain regions peaks around postnatal day 10 and declines thereafter [13]. The stronger effect of early postnatal downregulation is consistent with the peak of FMRP expression in microglia and the critical period (postnatal days 7–14 [26, 27] when microglia shape developing neuronal circuits through synaptic pruning and neurogenesis [28, 29]. Our results are consistent with previous studies linking microglia and FXS [12, 30]. Specifically, *Fmr1* KO mice display lower microglial density [31] and elevated reactivity of microglia to lipopolysaccharide, indicated by exaggerated phagocytosis and pro-inflammatory responses [19]. Our findings are also consistent with emerging evidence linking microglia to autism, including alterations in their number, morphology [17], and the

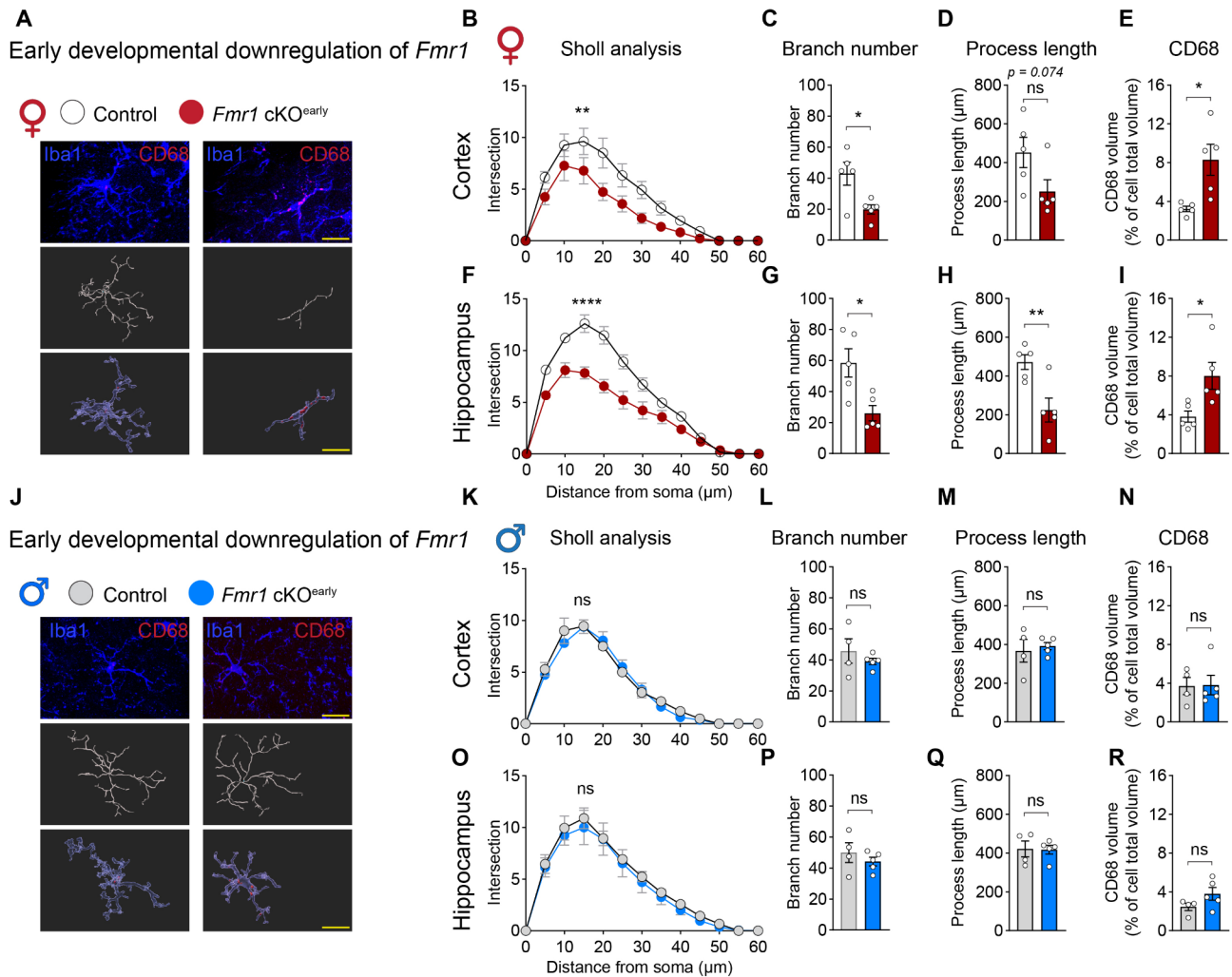


Fig. 3 Early developmental downregulation of microglial *Fmr1* causes morphological changes and enhances phagocytic activity. **(A)** Representative images, skeleton, and volumetric 3D reconstructions of microglia. **(B–I)** 3D analysis of Iba1⁺ microglia revealed that female *Fmr1* cKO^{early} microglia exhibit diminished arborization, as indicated by reduced number of intersections in 3D Sholl analysis **(B, cortex: $F_{12,96} = 2.52$, ** $p = 0.0062$ and F, hippocampus: $F_{12,96} = 14.90$, **** $p < 0.0001$)**, along with decreased branch number **(C, cortex: $t_8 = 2.90$, * $p = 0.0198$ and G, hippocampus: $t_8 = 3.12$, * $p = 0.0142$)** and processes length **(D, cortex: $t_8 = 2.04$, ns, $p > 0.074$ and H, hippocampus: $t_8 = 3.40$, ** $p = 0.0093$)**. Volumetric analysis of CD68 signal in microglia (Iba1⁺) showed a significant increase in CD68⁺/Iba1⁺ volume ratio in the cortex **(E, $t_8 = 3.11$, * $p = 0.0143$)** and hippocampus **(I, $t_8 = 2.78$, * $p = 0.0237$)** of female *Fmr1* cKO^{early} mice. Conversely, male *Fmr1* cKO^{early} mice exhibited no change in microglia morphology (representative reconstruction **(J)**), Sholl analysis **(K, O)**, branch number **(L, P)**, and processes length **(M, Q)** and phagocytosis capacity **(N, R)** in the cortex or hippocampus (Fig. 3J–R, ns, $p > 0.05$). Unpaired two-tailed Student's *t*-test was used for branch number, processes length, and CD68. For Sholl analysis, two-way ANOVA followed by Bonferroni's multiple comparisons test was used. The scale bars in A and J are 10 μ m. $n = 4–5$ mice/group. Data points represent individual mice. Data are shown as mean \pm SEM. * $p < 0.05$, ** $p < 0.01$, **** $p < 0.0001$, ns– not significant

expression of microglia-specific genes [32, 33] in post-mortem autistic brains, abnormalities in social behavior in mice with impaired microglia-mediated synaptic pruning, such as *Cx3cr1* KO [34], and the induction of behavioural phenotypes reminiscent of autism by maternal immune activation [35, 36].

Microglia exhibit sexual dimorphism in various physiological processes. Overexpression of eIF4E in microglia elevated mRNA translation in both sexes, but induced social deficits and increased microglial density and size in male mice only [37]. Conversely, single-cell RNA

sequencing of microglia in mouse models with high and normal anxiety-related behavior (HAB and NAB, respectively) revealed higher expression of genes associated with phagocytosis and synaptic engulfment in female HAB mice compared to males [38]. Accordingly, a greater amount of VGlut1⁺ excitatory synapses was engulfed by the female HAB microglia compared to the male microglia. Minocycline administration reduced synapse engulfment and anxiety-like behaviors in female but not male HAB mice [38]. Female-specific effects of *Fmr1* downregulation in microglia is an intriguing observation that

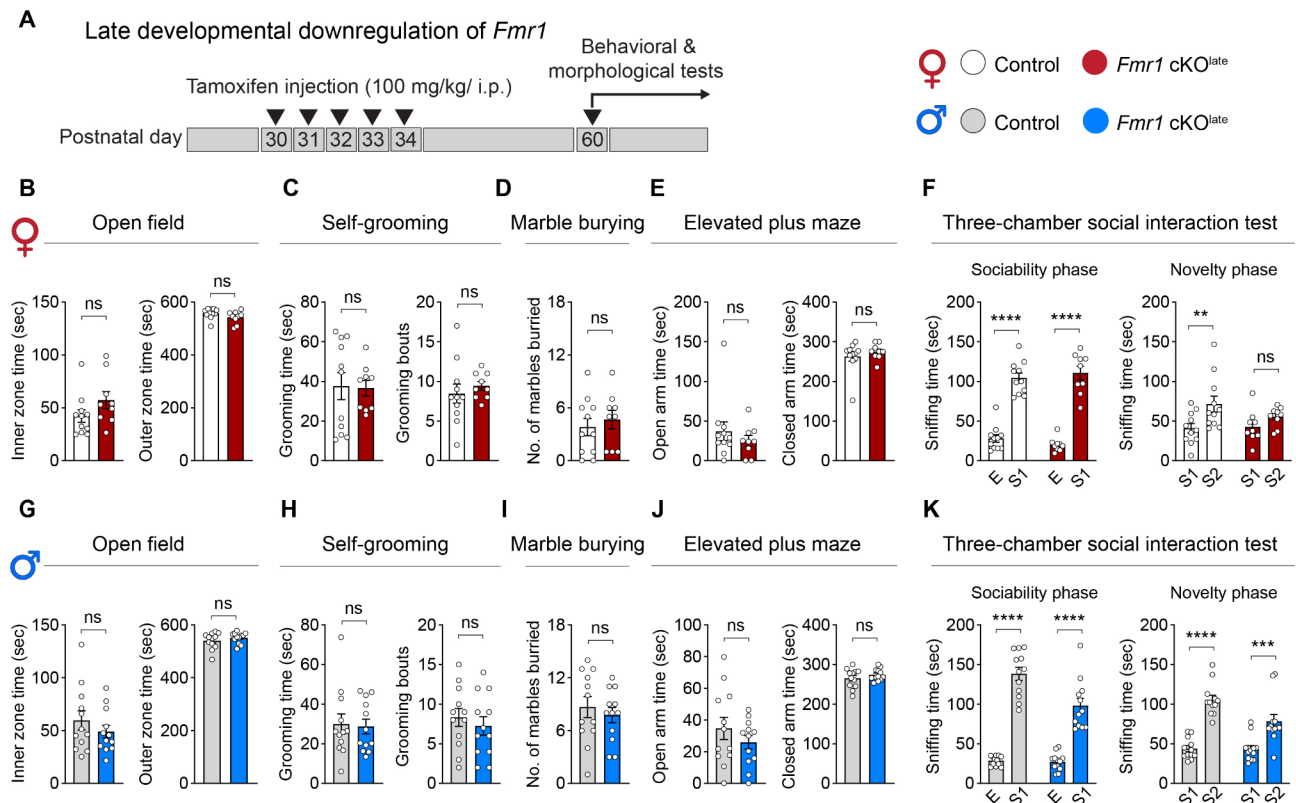


Fig. 4 Microglia-specific downregulation of *Fmr1* during late development leads to a deficit in novelty-seeking phase of the three-chamber social interaction test in female mice. **(A)** The schematic illustrates the late downregulation of the *Fmr1* gene in microglia. **(B–F)** The behavioral analysis of female *Fmr1* cKO^{late} mice ($n=9$) revealed impairment during novelty-seeking phase of the three-chamber social interaction test (**F**, right, $ns, p > 0.05$), but not during the sociability phase of the same test (**F**, left, $t_{36} = 10.31, ****p < 0.0001$). The female *Fmr1* cKO^{late} mice behaviors in the open field, self-grooming, marble burying, and elevated plus tests were comparable to the controls (**B–E**, $ns, p > 0.05$). The male *Fmr1* cKO^{late} mice did not show behavioral deficit during the open field, self-grooming, marble burying, and elevated plus tests in comparison to controls (**G–J**, $ns, p > 0.05$). The male *Fmr1* cKO^{late} mice did not exhibit impairment in sociability or novelty-seeking phases of the three-chamber social interaction test (**K**, $****p < 0.0001$ and $***p < 0.0001$ for empty cage **(E)** vs. stranger 1 (S1) and stranger 2 (S2) vs. stranger 1 (S1) in control and male *Fmr1* cKO^{late}). Unpaired two-tailed Student’s t-test was used for D, and **G–J**. Two-tailed Mann–Whitney test was used for B, C, and E. The three-chamber social interaction test was analyzed using two-way ANOVA followed by Bonferroni’s multiple comparisons test. Data points represent individual mice. Data are shown as mean \pm SEM. $**p < 0.01$, $***p < 0.001$, $****p < 0.0001$, ns – not significant

requires further investigation. There are several potential explanations for the observed sex differences. First, the number and characteristics of microglia vary between males and females in a region-specific and age-dependent manner [39]. Downregulation of *Fmr1* could differentially affect various brain regions, and accordingly, impact neuronal processes underlying complex behaviors in males and females. Second, the X chromosome contains a significant number of immune-related genes [39], raising the possibility that in the absence of *Fmr1*, X-linked immune-related genes may become dysregulated, preferentially affecting microglial homeostasis and function in females. Sex-specific effects might also be related to the interaction with sex hormones [40, 41] or alternatively, to the expression of TMEM119^{CreERT2} and the subsequent *Fmr1* downregulation in only a fraction of microglia [24, 42], raising the possibility that microglia

that do not undergo recombination compensate better in males than in females.

Limitations

This study investigated the effect of *Fmr1* downregulation in microglia on microglial morphology and distinct behaviors which are altered in *Fmr1* KO mice. Importantly, assessment of behaviors reminiscent of neurodevelopmental disorders, including autism, in mice is challenging [43] and requires additional tests to characterize alterations in sensory functions (vision, olfaction, touch), memory, and novelty detection [44]. We confirmed the downregulation of microglial FMRP expression in the corpus callosum, but not in other brain areas. This is because FMRP expression is substantially reduced to very low/undetectable levels in most brain regions by postnatal week 3, but remains readily detectable in the corpus callosum [13]. The TMEM119^{CreERT2} mouse line

is highly specific to microglia, without leakage of Cre activity [24]. Finally, we assessed microglia morphology and CD68 expression in the cortex and hippocampus. It will be important to examine other brain areas and additional behaviors that are affected in neurodevelopmental disorders.

Conclusion

This study found that *Fmr1* downregulation in microglia promotes microglial reactivity, enhances self-grooming behaviors and induces deficits in the novelty-seeking phase of the three-chamber social interaction test in female, but not male, mice. The exact mechanism by which FMRP-deficient microglia cause behavioral phenotypes remains unknown. While we assessed key phenotypes observed in *Fmr1* KO mice, other phenotypes, such as audiogenic seizures, dendritic spine morphology and density, LTD, protein synthesis, and the activity of different signaling cascades, should be investigated in future studies.

Abbreviations

FXS	Fragile X syndrome
FMRP	Fragile X messenger ribonucleoprotein
VGlut2	Vesicular-glutamate transporter 2
LTD	Long-term depression
GLT1	Glutamate transporter-1
ASD	Autism spectrum disorder
4-OHT	4-Hydroxytamoxifen
CD68	Cluster of differentiation 68

Supplementary Information

The online version contains supplementary material available at <https://doi.org/10.1186/s13229-025-00648-2>.

Supplementary Material 1: Fig.1: Early developmental downregulation of microglial *Fmr1* reduces reciprocal social interaction: (A)

Reciprocal (direct) social interaction was assessed in *Fmr1* cKO^{early} female mice. Unpaired two-tailed Student's t-test was used for the analysis. (B-D) Behavioral results of *Fmr1* cKO^{early} female and *Fmr1* cKO^{early} male mice from open field inner zone (Genotype: F (1, 30) = 1.213; $p = 0.2796$, Sex: F (1, 30) = 3.281; $p = 0.0801$, Interaction: F (1, 30) = 2.887; $p = 0.0960$), outer zone (Genotype: F (1, 30) = 1.213; $p = 0.2796$, Sex: F (1, 30) = 3.281; $p = 0.0801$, Interaction: F (1, 30) = 2.887; $p = 0.0960$), self-grooming (Genotype: F (1, 30) = 0.06116; $p = 0.8063$, Sex: F (1, 30) = 0.1492; $p = 0.7021$, Interaction: F (1, 30) = 5.383; $p = 0.0273^*$), and marble burying (F (1, 30) = 5.358; $p = 0.0276^*$, F (1, 30) = 0.1853; $p = 0.6699$, F (1, 30) = 6.778; $p = 0.0142^*$) tests were analysed together (analyses of each sex separately appear in Fig.2), using two-way ANOVA followed by Tukey's multiple comparisons test. P values for significant post-hoc comparisons are indicated on the graphs. (E) Reciprocal (direct) social interaction was assessed in *Fmr1* cKO^{late} female mice. Two-tailed Mann-Whitney test was used for the analysis. Data points represent individual mice. Data are shown as mean \pm SEM. ** $p < 0.01$, *** $p < 0.001$, **** $p < 0.0001$, ns– not significant.

Supplementary Material 2: Fig.2: The late developmental downregulation of *Fmr1* in microglia does not affect their morphology or phagocytic activity: (A, J) Representative images, skeleton, and volumetric 3D reconstructions of microglia. (B–I) 3D and volumetric analysis of Iba1⁺ microglia revealed no alterations in microglial arborization in female and male *Fmr1* cKO^{late} microglia as indicated by the unchanged number of 3D Sholl intersections, branch number, processes length, and no significant differences in phagocytic activity in cortex and hippocampus (ns, $p > 0.05$). Unpaired two-tailed Student's t-test was used for branch number,

processes length, and CD68. For Sholl analysis, a two-way ANOVA followed by Bonferroni's multiple comparisons test was used. The scale bars in A and J are 10 μ m. $n = 4$ –5 mice/group. Data points represent individual mice. Data are shown as mean \pm SEM. ns– not significant.

Acknowledgements

We thank Dr. David L. Nelson (Baylor College of Medicine, Houston) for kindly providing *Fmr1*^{fl/fl} mice.

Author contributions

M.H., C.G.G., and A.K. conceived the project, designed experiments, and supervised the research. M.H. performed immunohistochemistry and behavioral experiments, with the help of D.H.T., K.C.L., W.C., C.W., N.B., S.U., and J.F. N.S., V.H., and M.P.K. assisted with data interpretation. M.H., C.G.G., and A.K. wrote the manuscript with input from all the authors.

Funding

This work was supported by a grant from the Canadian Institutes of Health Research (CIHR, PJT-162412), the Azrieli Centre for Autism Research (ACAR) to A.K., and ERA-NET Neuron Sensory disorders project TRANSMECH (A.K. and C.G.G.). C.G.G. was supported by HFRI grant (Project No. 2556). M.H. was supported by the Brain Canada and Transforming Autism Care Consortium (TACC) graduate fellowships.

Data availability

No datasets were generated or analysed during the current study.

Declarations

Ethics approval

All procedures were compliant with the Canadian Council on Animal Care guidelines and approved by McGill University's Animal Care Committee.

Consent for publication

Not applicable.

Competing interests

The authors declare no competing interests.

Received: 21 June 2024 / Accepted: 3 February 2025

Published online: 07 March 2025

References

- Hunter J, Rivero-Arias O, Angelov A, Kim E, Fotheringham I, Leal J. Epidemiology of fragile X syndrome: a systematic review and meta-analysis. *Am J Med Genet A*. 2014;164A(7):1648–58.
- Hagerman RJ, Berry-Kravis E, Hazlett HC, Bailey DB, Moine H, Kooy RF, et al. Fragile X syndrome. *Nat Reviews Disease Primers*. 2017;3(1):1–19.
- Sethna F, Moon C, Wang H. From FMRP function to potential therapies for fragile X syndrome. *Neurochem Res*. 2014;39:1016–31.
- Gantois I, Khoutorsky A, Popic J, Aguilar-Valles A, Freemantle E, Cao R, et al. Metformin ameliorates core deficits in a mouse model of fragile X syndrome. *Nat Med*. 2017;23(6):674–7.
- Hooshmandi M, Sharma V, Perez CT, Sood R, Krimbacher K, Wong C, et al. Excitatory neuron-specific suppression of the integrated stress response contributes to autism-related phenotypes in fragile X syndrome. *Neuron*. 2023;111(19):3028–40. e6.
- Rais M, Lovelace JW, Shuai XS, Woodard W, Bishay S, Estrada L, et al. Functional consequences of postnatal interventions in a mouse model of Fragile X syndrome. *Neurobiol Dis*. 2022;162:105577.
- Lovelace JW, Rais M, Palacios AR, Shuai XS, Bishay S, Popa O, et al. Deletion of *Fmr1* from forebrain excitatory neurons triggers abnormal cellular, EEG, and behavioral phenotypes in the auditory cortex of a mouse model of fragile X syndrome. *Cereb Cortex*. 2020;30(3):969–88.
- Gonzalez D, Tomasek M, Hays S, Sridhar V, Ammanuel S, Chang C-w, et al. Audiogenic seizures in the *Fmr1* knock-out mouse are induced by *Fmr1* deletion in subcortical, VGlut2-expressing excitatory neurons and require deletion in the inferior colliculus. *J Neurosci*. 2019;39(49):9852–63.

9. Kalinowska M, van der Lei MB, Kitiashvili M, Mamcarz M, Oliveira MM, Longo F, et al. Deletion of Fmr1 in parvalbumin-expressing neurons results in dysregulated translation and selective behavioral deficits associated with fragile X syndrome. *Mol Autism*. 2022;13(1):29.
10. Koekkoek S, Yamaguchi K, Milojkovic B, Dortland B, Ruigrok T, Maex R, et al. Deletion of FMR1 in Purkinje cells enhances parallel fiber LTD, enlarges spines, and attenuates cerebellar eyelid conditioning in Fragile X syndrome. *Neuron*. 2005;47(3):339–50.
11. Pacey LK, Doering LC. Developmental expression of FMRP in the astrocyte lineage: implications for fragile X syndrome. *Glia*. 2007;55(15):1601–9.
12. D'Antoni S, Spatuzza M, Bonaccorso CM, Catania MV. Role of fragile X messenger ribonucleoprotein 1 in the pathophysiology of brain disorders: a glia perspective. *Neurosci Biobehav Rev*. 2024;162:105731.
13. Gholizadeh S, Halder SK, Hampson DR. Expression of fragile X mental retardation protein in neurons and glia of the developing and adult mouse brain. *Brain Res*. 2015;1596:22–30.
14. Higashimori H, Schin CS, Chiang MSR, Morel L, Shoneye TA, Nelson DL, et al. Selective deletion of astroglial FMRP dysregulates glutamate transporter GLT1 and contributes to fragile X syndrome phenotypes in vivo. *J Neurosci*. 2016;36(27):7079–94.
15. Bohlen CJ, Friedman BA, Dejanovic B, Sheng M. Microglia in brain development, homeostasis, and neurodegeneration. *Annu Rev Genet*. 2019;53:263–88.
16. Gehrmann J, Matsumoto Y, Kreutzberg GW. Microglia: intrinsic immunoeffector cell of the brain. *Brain Res Rev*. 1995;20(3):269–87.
17. Salter MW, Stevens B. Microglia emerge as central players in brain disease. *Nat Med*. 2017;23(9):1018–27.
18. Pardo CA, Vargas DL, Zimmerman AW. Immunity, neuroglia and neuroinflammation in autism. *Int Rev Psychiatry*. 2005;17(6):485–95.
19. Parrott J, Oster T, Lee H. Altered inflammatory response in FMRP-deficient microglia. *iScience*. 2021;24(11):103293.
20. Sekar A, Bialas AR, De Rivera H, Davis A, Hammond TR, Kamitaki N, et al. Schizophrenia risk from complex variation of complement component 4. *Nature*. 2016;530(7589):177–83.
21. Derecki NC, Cronk JC, Lu Z, Xu E, Abbott SB, Guyenet PG, et al. Wild-type microglia arrest pathology in a mouse model of Rett syndrome. *Nature*. 2012;484(7392):105–9.
22. Vargas DL, Nascimbene C, Krishnan C, Zimmerman AW, Pardo CA. Neuroglial activation and neuroinflammation in the brain of patients with autism. *Annals Neurology: Official J Am Neurol Association Child Neurol Soc*. 2005;57(1):67–81.
23. Mientjes E, Nieuwenhuizen I, Kirkpatrick L, Zu T, Hoogeveen-Westerveld M, Severijnen L-a, et al. The generation of a conditional Fmr1 knock out mouse model to study Fmrp function in vivo. *Neurobiol Dis*. 2006;21(3):549–55.
24. Kaiser T, Feng G. Tmem119-EGFP and Tmem119-CreERT2 transgenic mice for labeling and manipulating microglia. *Eneuro*. 2019;6(4).
25. Paolicelli RC, Sierra A, Stevens B, Tremblay M-E, Aguzzi A, Ajami B, et al. Microglia states and nomenclature: a field at its crossroads. *Neuron*. 2022;110(21):3458–83.
26. Guedes JR, Ferreira PA, Costa JM, Cardoso AL, Peça J. Microglia-dependent remodeling of neuronal circuits. *J Neurochem*. 2022;163(2):74–93.
27. Schafer DP, Lehrman EK, Kautzman AG, Koyama R, Mardinly AR, Yamasaki R, et al. Microglia sculpt postnatal neural circuits in an activity and complement-dependent manner. *Neuron*. 2012;74(4):691–705.
28. Dziabis JE, Bilbo SD. Microglia and sensitive periods in brain development. *Curr Top Behav Neurosci*. 2022;53:55–78. PMID: 34463934 https://doi.org/10.1007/7854_2021_242
29. Escoubas CC, Molofsky AV. Microglia as integrators of brain-associated molecular patterns. *Trends Immunol*. 2024;45(5):358–70.
30. Jawaid S, Kidd GJ, Wang J, Swetlik C, Dutta R, Trapp BD. Alterations in CA1 hippocampal synapses in a mouse model of fragile X syndrome. *Glia*. 2018;66(4):789–800.
31. Lee FH, Lai TK, Su P, Liu F. Altered cortical cytoarchitecture in the Fmr1 knock-out mouse. *Mol Brain*. 2019;12:1–12.
32. Suzuki K, Sugihara G, Ouchi Y, Nakamura K, Futatsubashi M, Takebayashi K, et al. Microglial activation in young adults with autism spectrum disorder. *JAMA Psychiatry*. 2013;70(1):49–58.
33. Voineagu I, Wang X, Johnston P, Lowe JK, Tian Y, Horvath S, et al. Transcriptomic analysis of autistic brain reveals convergent molecular pathology. *Nature*. 2011;474(7351):380–4.
34. Zhan Y, Paolicelli RC, Sforzini F, Weinhard L, Bolasco G, Pagani F, et al. Deficient neuron-microglia signaling results in impaired functional brain connectivity and social behavior. *Nat Neurosci*. 2014;17(3):400–6.
35. Estes ML, McAllister AK. Maternal immune activation: implications for neuropsychiatric disorders. *Science*. 2016;353(6301):772–7.
36. Erbescu A, Papuc SM, Budisteanu M, Arghir A, Neagu M. Re-emerging concepts of immune dysregulation in autism spectrum disorders. *Front Psychiatry*. 2022;13:1006612.
37. Xu Z-X, Kim GH, Tan J-W, Riso AE, Sun Y, Xu EY, et al. Elevated protein synthesis in microglia causes autism-like synaptic and behavioral aberrations. *Nat Commun*. 2020;11(1):1797.
38. Ugursu B, Sah A, Sartori S, Popp O, Mertins P, Dunay IR, et al. Microglial sex differences in innate high anxiety and modulatory effects of minocycline. *Brain Behav Immun*. 2024;119:465–81.
39. Han J, Fan Y, Zhou K, Blomgren K, Harris RA. Uncovering sex differences of rodent microglia. *J Neuroinflamm*. 2021;18:1–11.
40. Romano E, Cosentino L, Laviola G, De Filippis B. Genes and sex hormones interaction in neurodevelopmental disorders. *Neurosci Biobehav Rev*. 2016;67:9–24.
41. Garcia-Ovejero D, Azcoitia I, DonCarlos LL, Melcangi RC, Garcia-Segura LM. Glia-neuron crosstalk in the neuroprotective mechanisms of sex steroid hormones. *Brain Res Brain Res Rev*. 2005;48(2):273–86.
42. Bedolla AM, McKinsey GL, Ware K, Santander N, Arnold TD, Luo Y. A comparative evaluation of the strengths and potential caveats of the microglial inducible CreER mouse models. *Cell Rep*. 2024;43(1):113660.
43. Silverman JL, Thurm A, Ethridge SB, Soller MM, Petkova SP, Abel T, et al. Reconsidering animal models used to study autism spectrum disorder: current state and optimizing future. *Genes Brain Behav*. 2022;21(5):e12803.
44. Crawley JN. Twenty years of discoveries emerging from mouse models of autism. *Neurosci Biobehav Rev*. 2023;146:105053.

Publisher's note

Springer Nature remains neutral with regard to jurisdictional claims in published maps and institutional affiliations.